

Multiple fiber Bragg grating sensing system based on active mode-locking fiber laser

DELONG MENG¹, XIAOLEI YU², ZHIMIN ZHAO¹, SHILEI SHAN¹, HONGZHE LI¹

¹College of Science, Nanjing University of Aeronautics and Astronautics, Nanjing 210016, China

²Jiangsu Institute of Quality and Standardization, Nanjing 210029, China

In this paper, a new multiple fiber Bragg grating (FBG) sensing system based on active mode-locking fiber laser is proposed. The active mode-locking fiber laser is composed of a linear cavity with an Fabry–Perot laser diode (F-P LD) as a reflective cavity mirror, and the erbium-doped fiber as the gain medium. Meanwhile, the F-P LD is also used as the modulating element of the fiber laser. Multiple FBGs cascaded in a long fiber are used as both the sensors in the system and the components for wavelength selection in the active mode-locking fiber laser. The capacity of the proposed sensing system to interrogate multiple FBGs in wavelength and spatial domain is investigated. The proposed sensing system has the characteristics of low cost, good stability, good compatibility, and can be used in quasi-distributed multi-point sensing.

Keywords: fiber optics, Fabry–Perot laser diode, fiber laser, active mode-locking, fiber Bragg grating.

1. Introduction

Optical fiber sensing technology has attracted much attention due to its small size, strong anti-electromagnetic interference ability, low attenuation and good compatibility. It has been widely used in the measurement of temperature [1-3], strain [4-5], liquid level [6], refractive index, liquid concentration, acceleration and so on. Optical fiber sensing technology can be divided into point type and distributed optical fiber sensing technology according to whether it is sustainable. Fiber Bragg grating sensors and optical fiber microstructure inter-mode interference sensors are single-point optical fiber sensors [7], and they can measure a variety of physical parameters. With the continuous advancement of optical fiber sensing technology, the range of perceivable physical quantities has become broader. The measurement range in the actual application is no longer limited to point sensing, but a large regional range. Therefore, the distributed optical fiber sensing technology which can realize large-scale measurement has been developed rapidly. Distributed optical fiber sensing technology mainly includes quasi-distributed optical fiber sensing technology [8-10] and fully distributed optical fiber sensing technology [11-13]. Both of them have high sensitivity and accuracy, and they

can perform real-time multi-point measurement. Therefore, they have high application value of civil engineering, chemical monitoring and analysis, and geological disaster monitoring.

Fiber Bragg gratings are widely used in optical fiber sensing as one of the most important sensing devices, the sensing information is obtained by analyzing the wavelength shift of FBG. The advantage of FBGs as sensors, compared to other sensors, is that the absolute wavelength coding, which is not affected by system loss and light source power fluctuations. Multi-FBG sensing is an attractive technique [14-15], because it can better utilize the advantages of FBGs, and achieve quasi-distributed optical fiber sensing. Multi-FBG interrogation is a key aspect for multi-FBG sensing, and wavelength-division multiplexing and spatial-division multiplexing are the two basic techniques. Wavelength-division multiplexing can make full use of the power for the broadband light source and improve the signal-to-noise ratio (SNR) of the system. However, the bandwidth of the light source and the detector limits the number of sensors, and it will increase the interrogation cost of the system. The advantage of spatial-division multiplexing is that the FBG sensors of each channel will not interfere with each other, which will improve the signal-to-noise. But the power utilization of the light source is low. Besides, the use of scanning Fabry–Perot filters [16, 17] matched grating filters [18] and other optical filters can also achieve the interrogation for multi-FBG sensing. However, these systems not only have low use efficiency for light source, resulting in low signal-to-noise ratio, but also cannot distinguish the FBGs at different positions along the fiber. In this regard, KERSEY and MOREY made an initial proposal to determine the spatial location of FBGs [19]. More recently, CHEN *et al.* used Fourier domain mode-locked fiber laser to achieve the positioning and interrogation for multi-FBGs [20]. Because the interrogation for multi-FBG sensing is achieved by using the Fabry–Perot tunable filter, the resolution of the system will be limited by the slow tuning speed of the Fabry–Perot tunable filter. To solve the problem, MADRIGAL *et al.* proposed a multi-FBG sensing system based on fiber ring laser [21], however, the system needs to rely on expensive optical components and this will increase the cost of the system.

In this paper, a new multi-FBG sensing system based on active mode-locking fiber laser is proposed, and the resonant cavity of the laser is formed by an Fabry–Perot laser diode and FBGs. With the filtering characteristics of FBGs, active mode-locking is achieved by modulating the Fabry–Perot laser diode. The F-P LD is utilized both as a modulator and a reflection cavity mirror of the fiber laser in the proposed system. In addition, when driving below the threshold, the F-P LD exhibits multi-mode property and its function is equivalent to a comb filter. Thus, the F-P LD also plays the role of a tunable comb filter, which greatly reduces the cost of the system. Meanwhile, the mode-locking operation of the fiber laser offers a convenient way to determine the spatial positions of the FBGs. The wavelength and spatial domain interrogations for multi-FBG are achieved, and it can be used in quasi-distributed multi-point sensing.

Section 2 introduces the structure and working principle of the sensing system. Section 3 describes the experimental process of the system. The results and analysis to

prove the working principle are presented, and the system is verified with temperature sensing. Finally, Section 4 summarizes the conclusions obtained.

2. Experimental structure and principle

The structure of the multi-FBG sensing system based on active mode-locking fiber laser is shown in Fig. 1. The active mode-locking fiber laser is composed of a linear cavity, which is made of a section of erbium-doped fiber and two reflecting cavity mirrors. One of the mirrors is the F-P LD, and the other is each sensing FBG. The 980 nm pump light enters the cavity through wavelength-division multiplexing (WDM) to pro-

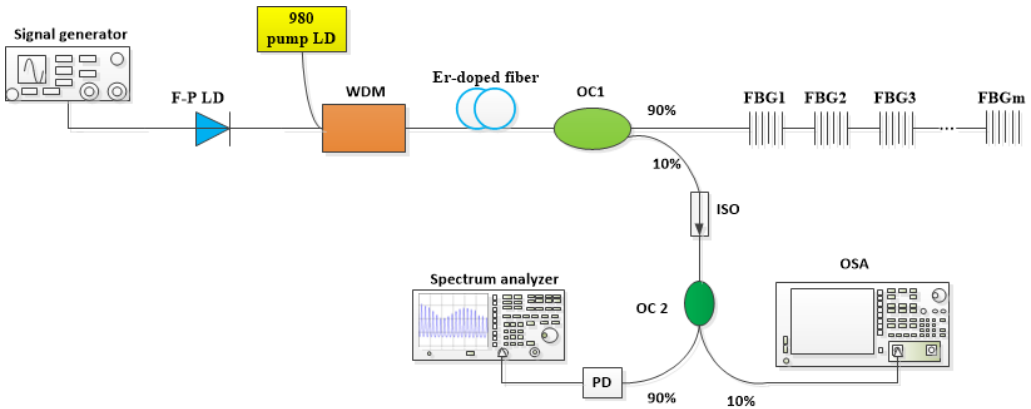


Fig. 1. Structure diagram of multi-FBG sensing system based on active mode-locking fiber laser. WDM: wavelength division multiplexer; OC: optical coupler; OSA: optical spectrum analyzer; PD: photo-detector; ISO: optical fiber isolator.

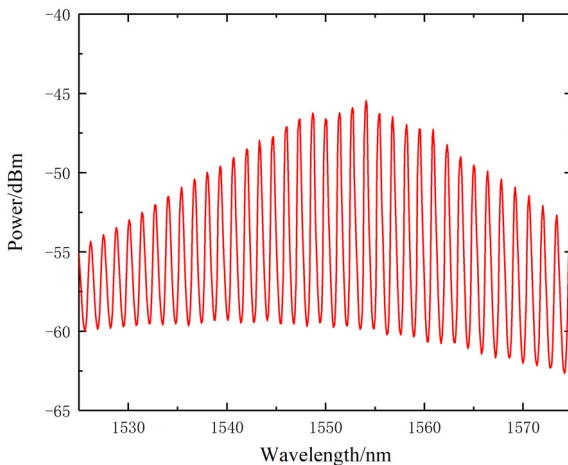


Fig. 2. Spectrum of F-P LD observed on the optical spectrum analyzer.

vide stable gain for the fiber laser. The optical spectrum of the fiber laser is observed by an optical spectrum analyzer (OSA), and multiple longitudinal mode beat frequency is generated in the resonant cavity. The beat frequency signals can be observed on the spectrum analyzer through a photo-detector (PD). In the experiment, the driving for the F-P LD is adjusted to below the threshold to ensure that no laser can be emitted, and its function is equivalent to a tunable comb filter. The optical spectrum of F-P LD observed on the optical spectrum analyzer is shown in Fig. 2.

The fundamental frequency of the laser cavity can be adjusted by the FBGs, and it can be expressed as

$$f = \frac{c}{2nL} \quad (1)$$

where c is the velocity of light in a vacuum, n is the effective refractive index of fiber, and L is the length of the laser resonant cavity.

The active mode-locking of the system is realized by loading resonant frequencies corresponding to resonant cavities of different lengths, so that the output of the fiber laser is at a certain wavelength, which is corresponding to the FBGs at different positions. Therefore, the positioning of multi-FBG sensors is achieved by active mode-locking. In theory, this principle can be applied to m FBGs. However, due to the harmonic frequencies of the resonant cavity in the system, it may limit the number of FBGs which can be detected in the system.

The principle of active mode-locking is shown in Fig. 3. The intensity modulation is adopted to achieve the active mode-locking, an external sinusoidal radio frequency signal is added to the F-P LD, and a sinusoidal optical loss modulation with the same frequency as the modulation frequency is formed in the cavity. When the modulation frequency is matched to the longitudinal mode spacing of the resonant cavity, the saturable gain in the cavity will produce a net gain that is close to the minimum modulation loss, resulting in an ultrashort pulse. When the modulation frequency is an integer multiple of the fundamental frequency, it can also generate a mode-locking pulse with the same repetition frequency as the modulation frequency of the laser.

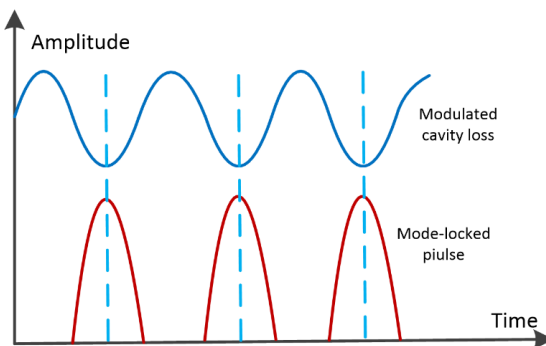


Fig. 3. Schematic diagram of active mode-locking operation.

3. Experimental results and discussion

Three FBGs are selected as the test objects with the wavelengths corresponding to the output spectrum of the F-P LD. The center wavelengths of the three fiber Bragg gratings are 1547.03, 1549.05, and 1554.08 nm; the reflectivities are 90%, 94.37%, and 93.45%, respectively. The spectra of the three FBGs is shown in Fig. 4. In the experiment, the distance between the F-P LD and FBGs (FBG1, FBG2, FBG3) are 47.3, 48.3, and 49.3 m, according to the Eq. (1). The resonant frequencies of the active mode-locking laser are 2.11, 2.07, and 2.03 MHz.

Initially, adjust the pump power to 23.5 mW, and the F-P LD is modulated with sinusoidal signals of different frequencies. As it is expected, when the modulation fre-

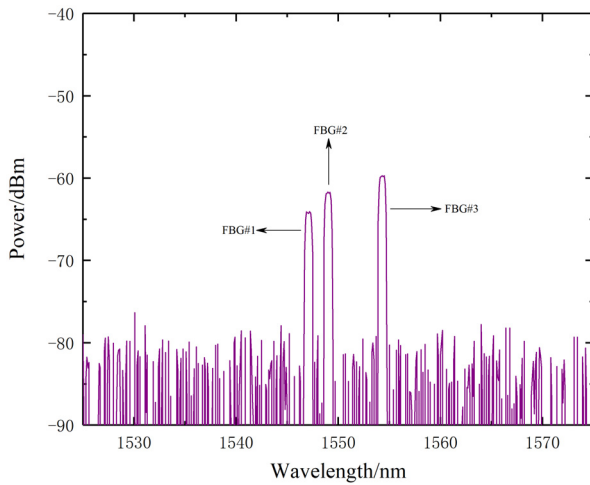


Fig. 4. Spectra of the FBGs under test.

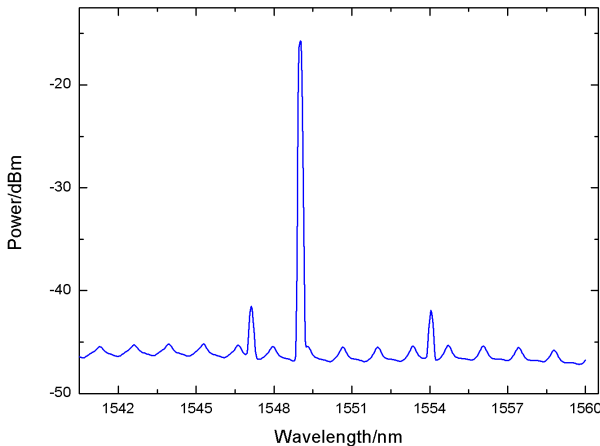


Fig. 5. Spectrum observed when the modulation frequency is 2.07 MHz.

quency is different from the resonant frequencies, there is no peak or its power is very low, but when the modulation frequency is matched to one of the resonant frequencies, a significant peak at the corresponding FBG wavelength is observed on the spectrum analyzer, and the laser is working in the mode-locking state. The spectrum of the active mode-locking is obtained when the modulation frequency is 2.07 MHz, and it is shown in Fig. 5. It can be seen that the peak wavelength of the output is about 1549.05 nm, and the signal-to-noise ratio is about 32 dB.

Then the experiments for three selected fiber Bragg gratings are conducted. Figure 6 shows the spectra observed on the optical spectrum analyzer at different modulation frequencies (2.03, 2.07, and 2.11 MHz). It can be seen that the outputs of the laser all have a better signal-to-noise ratio. The results showed that the active mode-locking of the system is realized by modulating the F-P LD, and the capacity of the system to interrogate multi-FBG in spatial domain is confirmed.

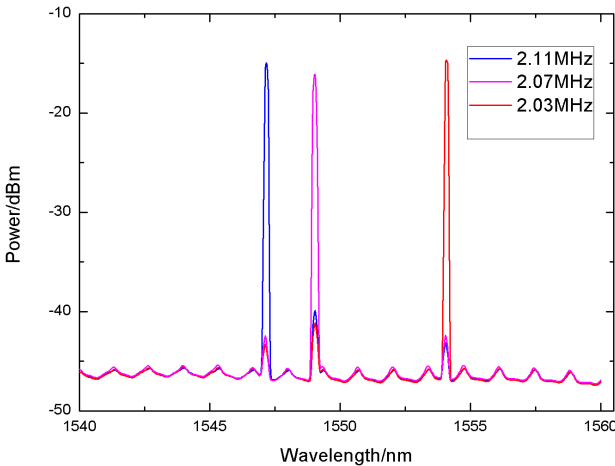


Fig. 6. Spectra observed at different modulation frequencies.

In order to verify whether the selected cavity is a mode-locking laser, the beat frequency spectrum of the output signal is measured. In order to make the system stable, in the experiment, a section of unpumped erbium-doped fiber is selected as a saturable absorber, which is used to selectively absorb some modes of the resonant cavity. Meanwhile, the appropriate 980 nm pump power is selected, which is slightly higher than the threshold to achieve the purpose of stabilizing the signal. Figure 7 shows the beat frequency spectrum when the modulation frequency is 2.07 MHz applied to the F-P LD. The spectrum clearly shows the fundamental frequency at 2.07 MHz and its harmonic frequencies, which shows the periodicity of the pulsed optical signal. The experimental results are agreed with the theoretical value, which proves that the target cavity does work under the expected mode-locking regime, while the other cavities do not.

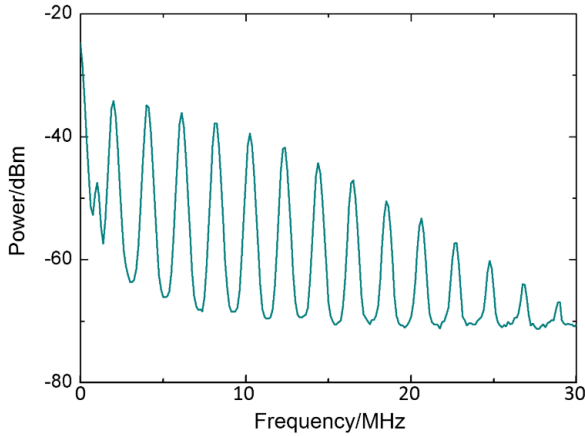


Fig. 7. Electrical spectrum of the photo-detected signal when the modulation frequency is 2.07 MHz.

A temperature sensing experiment is conducted to verify the system. In order to prevent the external temperature from affecting the output results, ensure that the minimum sensing temperature is higher than the current indoor temperature. The sensing FBG (FBG2) is placed in a constant temperature box, the temperature controller was employed to control the FBG sensing temperature with a step of 5 °C, and the temperature is gradually increased from 25 to 55 °C. The shift of the wavelength is recorded, the measured results are shown in Fig. 8. It can be seen that with the temperature increase, the center wavelength of the sensing fiber Bragg grating increases.

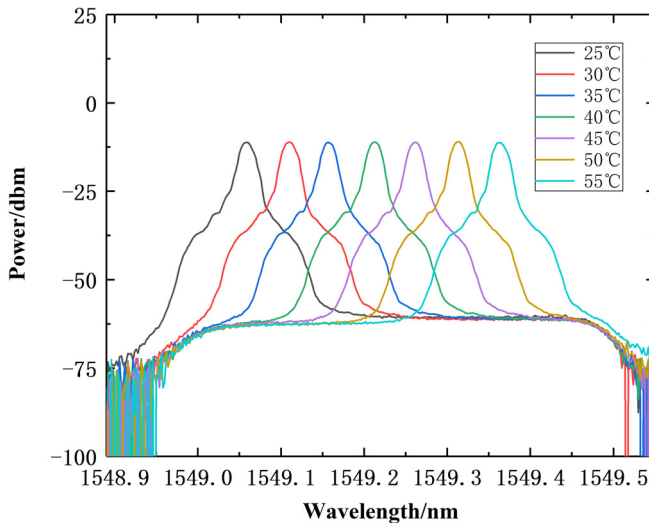


Fig. 8. Laser output spectral lines under different temperatures.

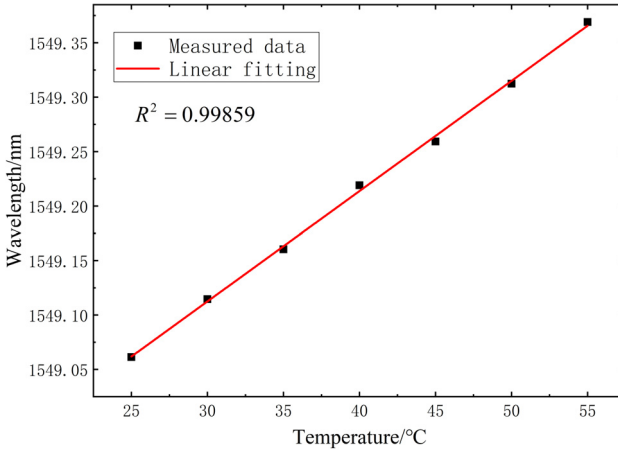


Fig. 9. Fitting line of wavelength at different temperatures.

The relationship between the wavelength of the FBG and temperature is shown in Fig. 9. It shows that the wavelength varied linearly with the temperature with a fitting degree of 99.859%, and it corresponds to an FBG sensor with a temperature coefficient of 9.9 pm/°C.

4. Conclusion

In conclusion, a new multi-fiber Bragg grating sensing system based on active mode-locking fiber laser is proposed. In the proposed system, the F-P LD is not only used as a mirror but also as a modulator in the active mode-locking laser, which greatly reduces the cost of the system. Simultaneously, the system can interrogate the spatial positions of the FBGs placed in series along the fiber by setting the modulation frequency to each value of the FBG resonance frequencies. The limitation of the system is that the wavelength of the selected fiber Bragg grating should be corresponding to the output optical spectrum of the F-P LD. Finally, a temperature sensing experiment is conducted to verify the system. The results showed that the system can interrogate the FBG when the FBG is wavelength shifted. The proposed system has the advantages of low cost, simple structure and good stability.

Acknowledgment

The work was financially supported by the National Natural Science Foundation of China (No. 61771240) and the Six Talent Peaks Project in Jiangsu Province of China (XYDXX-058).

References

- [1] DING W., JIANG Y., GAO R., LIU Y., *High-temperature fiber-optic Fabry–Perot interferometric sensors*, *Review of Scientific Instruments* **86**(5), 2015, 055001, DOI: [10.1063/1.4919409](https://doi.org/10.1063/1.4919409).

- [2] LI W.C., YUAN Y.G., YANG J., YUAN L.B., *In-fiber integrated high sensitivity temperature sensor based on long Fabry–Perot resonator*, Optics Express **27**(10), 2019, pp. 14675–14683, DOI: [10.1364/OE.27.014675](https://doi.org/10.1364/OE.27.014675).
- [3] WANG X., CHEN T.W., MENG D.L., WANG F., *A simple FBG Fabry–Perot sensor system with high sensitivity based on fiber laser beat frequency and Vernier effect*, IEEE Sensors Journal **21**(1), 2020, pp. 71–75, DOI: [10.1109/JSEN.2020.2974501](https://doi.org/10.1109/JSEN.2020.2974501).
- [4] LIU Y., WANG D.N., *Fiber in-line Fabry–Perot interferometer with offset splicing for strain measurement with enhanced sensitivity*, IEEE Photonics Journal **10**(1), 2018, 7100708, DOI: [10.1109/JPHOT.2017.2739198](https://doi.org/10.1109/JPHOT.2017.2739198).
- [5] LIU S., WANG Y., LIAO C., WANG G., LI Z., WANG Q., ZHOU J., YANG K., ZHONG X., ZHAO J., TANG J., *High-sensitivity strain sensor based on in-fiber improved Fabry–Perot interferometer*, Optics Letters **39**(7), 2014, pp. 2121–2124, DOI: [10.1364/OL.39.002121](https://doi.org/10.1364/OL.39.002121).
- [6] Wang D., Zhang Y., Jin B.Q., Wang Y., Zhang M.J., *Quasi-distributed optical fiber sensor for liquid-level measurement*, IEEE Photonics Journal **9**(6), 2017, 6805107, DOI: [10.1109/JPHOT.2017.2776245](https://doi.org/10.1109/JPHOT.2017.2776245).
- [7] Hu D.T., Lv S.K., Guo Y.X., He H.G., Liu J.Y., *A fiber Bragg grating force sensor with sensitization structure*, IEEE Sensors Journal **21**(3), 2021, pp. 3042–3048, DOI: [10.1109/JSEN.2020.3027569](https://doi.org/10.1109/JSEN.2020.3027569).
- [8] ZHENG Y., ZHU Z.W., XIAO W., GU D.M., DENG Q.X., *Investigation of a quasi-distributed displacement sensor using the macro-bending loss of an optical fiber*, Optical Fiber Technology **55**, 2020, 102140, DOI: [10.1016/j.yofte.2020.102140](https://doi.org/10.1016/j.yofte.2020.102140).
- [9] GAO X., WANG G., ZHAI C., et al., *Quasi-distributed optical fiber liquid leakage sensors based on lateral coupling structure*, Optical Technique **45**(4), 2019, pp. 453–457.
- [10] XIANG Y., LUO Y., LI Y., LI Y., YAN Z.J., LIU D.M., SUN Q.Z., *Quasi-distributed dual-parameter optical fiber sensor based on cascaded microfiber Fabry–Perot interferometers*, IEEE Photonics Journal **10**(2), 2018, 2400309, DOI: [10.1109/JPHOT.2018.2817573](https://doi.org/10.1109/JPHOT.2018.2817573).
- [11] WANG C.J., LI Z.Y., GUI X., FU X.L., WANG F., WANG H.H., WANG J.Q., BAO X.Y., *Micro-cavity array with high accuracy for fully distributed optical fiber sensing*, Journal of Lightwave Technology **37**(3), 2019, pp. 927–932, DOI: [10.1109/JLT.2018.2883824](https://doi.org/10.1109/JLT.2018.2883824).
- [12] WANG D.Y., WANG Y.M., MING H., GONG J.M., WANG A., *Fully distributed fiber-optic biological sensing*, IEEE Photonics Technology Letters **22**(21), 2010, pp. 1553–1555, DOI: [10.1109/LPT.2010.2069089](https://doi.org/10.1109/LPT.2010.2069089).
- [13] WANG D.Y., WANG Y., GONG J., WANG A., *Fully distributed fiber-optic temperature sensing using acoustically-induced rocking grating*, Optics Letters **36**(17), 2011, pp. 3392–3394, DOI: [10.1364/OL.36.003392](https://doi.org/10.1364/OL.36.003392).
- [14] XIE F., ZHANG S.L., LI Y., LEE S.B., *Multiple in-fiber Bragg gratings sensor with a grating scale*, Measurement **31**(2), 2002, pp. 139–142, DOI: [10.1016/S0263-2241\(01\)00038-0](https://doi.org/10.1016/S0263-2241(01)00038-0).
- [15] XIE F., ZHANG S.L., LI Y., LEE S.B., *Temperature-compensating multiple fiber Bragg grating strain sensors with a metrological grating*, Optics and Lasers in Engineering **41**(1), 2004, pp. 205–216, DOI: [10.1016/S0143-8166\(02\)00145-8](https://doi.org/10.1016/S0143-8166(02)00145-8).
- [16] ZHANG X., NIU H., HOU C., DI F., *An edge-filter FBG interrogation approach based on tunable Fabry–Perot filter for strain measurement of planetary gearbox*, Optical Fiber Technology **60**, 2020, 102379, DOI: [10.1016/j.yofte.2020.102379](https://doi.org/10.1016/j.yofte.2020.102379).
- [17] ZHAN Y., LIN F., SONG Z., SUN Z., YU M., *Applications and research progress of optical fiber grating sensing in thermoplastic composites molding and structure health monitoring*, Optik **229**, 2021, 166122, DOI: [10.1016/j.ijleo.2020.166122](https://doi.org/10.1016/j.ijleo.2020.166122).
- [18] CHAN C. C., GONG J.M., SHI C.Z., JIN W., ZHANG M., ZHOU L.M., DEMOKAN M.S., *Improving measurement accuracy of fiber Bragg grating sensor using digital matched filter*, Sensors and Actuators A: Physical **104**(1), 2003, pp. 19–24, DOI: [10.1016/S0924-4247\(02\)00437-5](https://doi.org/10.1016/S0924-4247(02)00437-5).
- [19] KERSEY D., MOREY W.W., *Multiplexed Bragg grating fibre-laser strain-sensor system with mode-locked interrogation*, Electronics Letters **29**(1), 1993, pp. 112–114, DOI: [10.1049/el:19930073](https://doi.org/10.1049/el:19930073).

- [20] CHEN D., SHU C., HE S., *Multiple fiber Bragg grating interrogation based on a spectrum-limited Fourier domain mode-locking fiber laser*, Optics Letters **33**(13), 2008, pp. 1395–1397, DOI: [10.1364/OL.33.001395](https://doi.org/10.1364/OL.33.001395).
- [21] MADRIGAL J., FRAILE-PELÁEZ F.J., ZHENG D., BARRERA D., SALES S., *Characterization of a FBG sensor interrogation system based on a mode-locked laser scheme*, Optics Express **25**(20), 2017, pp. 24650–24657, DOI: [10.1364/OE.25.024650](https://doi.org/10.1364/OE.25.024650).

*Received May 22, 2021
in revised form July 17, 2021*